5-1-1994

Tabletop X-ray Lasers

D. C. Eder
Lawrence Livermore National Laboratory

P. Amendt
Lawrence Livermore National Laboratory

L. B. DaSilva
Lawrence Livermore National Laboratory

R. A. London
Lawrence Livermore National Laboratory

B. J. MacGowan
Lawrence Livermore National Laboratory

See next page for additional authors

Tabletop xray lasers@f|

D. C. Eder, P. Amendt, L. B. DaSilva, R. A. London, B. J. MacGowan et al.

Citation: Phys. Plasmas **1**, 1744 (1994); doi: 10.1063/1.870936
View online: http://dx.doi.org/10.1063/1.870936
View Table of Contents: http://pop.aip.org/resource/1/PHPAEN/v1/i5
Published by the AIP Publishing LLC.

Tabletop x-ray lasers*

D. C. Eder,† P. Amendt, L. B. DaSilva, R. A. London, B. J. MacGowan, D. L. Matthews, B. M. Penetrante, M. D. Rosen, and S. C. Wilks
Lawrence Livermore National Laboratory, Livermore, California 94550

T. D. Donnelly and R. W. Falcone
University of California at Berkeley, Berkeley, California 94720

G. L. Strobel
University of Georgia, Athens, Georgia 30602

(Received 8 November 1993; accepted 12 January 1994)

Details of schemes for two tabletop size x-ray lasers that require a high-intensity short-pulse driving laser are discussed. The first is based on rapid recombination following optical-field ionization. Analytical and numerical calculations of the output properties are presented. Propagation in the confocal geometry is discussed and a solution for x-ray lasing in Li-like N at 247 Å is described. Since the calculated gain coefficient depends strongly on the electron temperature, the methods of calculating electron heating following field ionization are discussed. Recent experiments aimed at demonstrating lasing in H-like Li at 135 Å are discussed along with modeling results. The second x-ray laser scheme is based on the population inversion obtained during inner-shell photoionization by hard x rays. This approach has significantly higher-energy requirements, but lasing occurs at very short wavelengths ($\lambda \leqslant 15$ Å). Experiments that are possible with existing lasers are discussed.

I. INTRODUCTION

The development of low cost *tabletop* size x-ray lasers is critical if x-ray lasers are to become as common a laboratory tool as infrared, optical, and ultraviolet lasers. The major factor that makes the cost of x-ray lasers prohibitively high for small laboratory operation is the size and cost of the driving laser. With this in mind, the primary objective of this paper is to discuss an approach to tabletop x-ray lasing based on recombination following optical-field ionization of a plasma by a high-intensity short-pulse driving laser.[1–8] We summarize the extensive theoretical work that has been done on this optical-field-ionized (OFI) x-ray laser scheme and discuss some recent experiments that have obtained some very promising results. In addition, we discuss an x-ray scheme based on inner-shell photoionization (ISPI) that also requires a high-intensity short-pulse driving laser.[9–11] The ISPI scheme requires driving lasers with energies approximately a factor of 10 greater than what is available currently, but would operate at wavelengths significantly shorter than current x-ray lasers.

The majority of current x-ray lasers reach the desired ionization state through collisions with free electrons heated by a large optical driving laser.[12] While advances in technology are reducing the size and cost for the required driving lasers,[13] they are still out of the range of most universities and small research laboratories. Even with advances that would allow 1–5 kJ lasers to fit on large optical tables, the x-ray laser schemes using these lasers are better referred to as laboratory-size rather than tabletop size systems.

In contrast, the proposed OFI x-ray laser has small enough energy requirements to be called a tabletop system. The major reason for the reduced energy requirements is that the oscillatory electric field associated with the driving laser ionizes the x-ray lasing plasma directly, rather than indirectly, through free-electron collisions. Optical field ionization occurs when the oscillatory electric field becomes comparable to the Coulomb field, holding the electrons to the nucleus.[14] An efficient way to have a long length of atoms/ions exposed to the large electric field is to use a confocal geometry allowing for a spot focus rather than the conventional line focus used in transverse pumping. The density of the lasant material is sufficiently low, such that depletion of the driving laser pulse is usually not an issue, except for very short ($\Delta t < 50$ fs) pulses. The low input energy requirements ($E_{in} \leqslant 1$ J) of this x-ray laser scheme allow for the possibility of high repetition rates (10–1000 Hz). High repetition rates are critical for most pump/probe experiments, and for many material science experiments, such as photoelectron spectroscopy.[15]

The ISPI approach to x-ray lasing also requires a high-intensity short-pulse driving laser, but has significantly higher input energy requirements because the ionization mechanism is more indirect than the OFI scheme, or even conventional collisional x-ray laser schemes. For the ISPI scheme, the inner-shell ionization is by incoherent x rays emitted from a nearby plasma that is heated and ionized by free electrons that obtain their energy from the driving laser. The advantage of the ISPI approach is that very short-wavelength ($\lambda \leqslant 15$ Å) x-ray lasing is possible.[10,11] Such short wavelengths are not possible with current collisional excitation x-ray laser schemes, where 35 Å in Ni-like Au is the shortest wavelength observed to lase.[12] In fact, the shortest possible wavelength in this scheme is only

*Paper 9I3, Bull. Am. Phys. Soc. **38**, 2099 (1993).
†Invited speaker.

 1070-664X/94/1(5)/1744/9/$6.00

21.5 Å, with Ni-like U. Short wavelengths are not possible with the OFI approach because of excessive electron heating when the scheme is extended to wavelengths of order 50 Å or shorter by using higher Z ions that require higher intensities.[5,6] In this paper, we discuss what aspects of ISPI x-ray lasers can be studied with existing short-pulse lasers.

There are other approaches to tabletop lasing using high-intensity short-pulse drivers that we mention briefly here. For example, one approach is a variation of conventional recombination x-ray lasers using microspheres that expand and cool rapidly.[16] In addition, there are approaches that do not utilize high-intensity short-pulse drivers. For example, there has been recent work on extending Ni-like schemes to longer wavelengths using a series of relatively low-intensity 100 ps pulses.[17] There has also been work on using capillary discharges as compact x-ray laser sources.[18,19] More information on x-ray lasing and tabletop approaches is given in the proceedings of recent conferences.[12,20]

A review of OFI x-ray lasing is given in Sec. II. In Sec. II A, we calculate the output property of OFI x-ray lasers and discuss appropriate applications. We discuss ionization-induced refraction and a potential solution using large focal spots in Sec. II B. Calculations of electron heating following field ionization are discussed in Sec. II C. In Sec. II D, we discuss recent experiments in H-like Li at 135 Å. The inner-shell photoionization approach is discussed in Sec. III, with the role of filters and electron moderators described in Sec. III A. The saturation intensity and output property of ISPI lasers are presented in Sec. III B. Experiments utilizing existing laser technology for addressing important aspects of ISPI lasing are discussed in Sec. III C. A summary with the prospects for tabletop lasing is given in Sec. IV.

II. OPTICAL-FIELD-IONIZED PLASMA SCHEMES

The OFI approach to x-ray lasing utilizes the rapid recombination following field ionization by a high-intensity short-pulse laser. One major difference of OFI plasma x-ray lasing compared to conventional recombination lasing is that cooling is not required because field ionization can produce low-energy rapidly recombining electrons.[21,22] Calculations predict x-ray lasing with large gain coefficients during such fast recombination.[4–8] Another major difference of the OFI approach is that lasing can occur down to the ground state of the ion with H- and Li-like ions of primary interest.

The advantage of lasing to the ground state is that the energy of the lasing transition is relatively large, compared to lasing between excited states. However, a very complete emptying of the ground state during ionization is required because the upper-laser state can never have a very large population due to the rapid radiative rate down to the ground state. Calculations show that a fractional population of 10^{-3} or greater remaining in the ground state can significantly reduce the predicted gain.[6] However, ionization is a strong function of the intensity, and calculations show that only a modest increase in intensity above the multiphoton thereshold is required to obtain nearly complete ionization.[14] A disadvantage of lasing to the ground state is that electrons have slow exit channels out of the ground state resulting in a short duration of lasing and a reduction in the saturation intensity. Both of these factors reduce the energy that can be obtained from the laser. First, we address what output energy one would expect from the laser if saturation is obtained and what are some of the potential applications. We then discuss propagation, electron heating, and some recent experimental results.

A. Saturated output energy and potential applications

For a proposed x-ray laser scheme to be of significant interest, the output energy must be high enough to be of use for the intended applications. The output energy at saturation is approximately equal to the product of the saturation intensity, the duration of lasing, and the cross-sectional area of the lasing region. We consider first the saturation intensity for OFI plasma x-ray lasers. A property of all lasers is that the output intensity increases exponentially with length until saturation is reached, whereupon the dependence on length becomes nearly linear. The saturation intensity $I_{\rm sat}$ is defined as the intensity at which the gain is reduced to one-half the small-signal-gain value. The saturation intensity for the OFI laser scheme has been studied both analytically[5,6,23] and numerically.[7] We first discuss a simple analytical method to determine $I_{\rm sat}$ and then comment on the numerical approach.

The gain coefficient g_{mn} for a transition between upper level m and lower level n varies with time, and can be written as

$$g_{mn}(t)=\frac{c^2}{4\pi^2\nu_{mn}^2}\frac{A_{mn}}{\Delta\nu_{mn}}\Delta N(t), \tag{1}$$

where $\Delta N(t)=[N_m(t)-N_n(t)h_m/h_n]$ is the population inversion density, $h_{m(n)}$ is the upper (lower) degeneracy, ν_{mn} is the frequency of the lasing transition, $\Delta\nu_{mn}$ is the line width that is usually determined by Stark broadening,[24] and $A_{mn}=8\pi^2e^2\nu_{mn}^2(f_{mn})^{\rm em}/m_ec^3$ is the radiative decay rate, with $(f_{mn})^{\rm em}$ being the emission oscillator strength. The small-signal-gain coefficient is given by the above expression when the populations are not affected by stimulated emission. Let Γ_0 be the flow rate per atom out of the upper-lasing level, including only nonstimulated processes. Next, define a parameter α, such that $\alpha\Gamma_0$ is the net stimulated emission rate per atom under saturation intensity conditions out of the upper-lasing level:

$$\alpha\Gamma_0=A_{mn}\frac{c^2}{2h\nu_{mn}^3}\left(1-\frac{N_n'h_m}{N_m'h_n}\right)J_{\rm sat}, \tag{2}$$

where $J_{\rm sat}$ is the specific mean saturation intensity per steradian.[6] The populations of the levels at saturation are denoted with primes, and we have dropped the explicit time dependence. Equating the small-signal outward flow from the upper-lasing level to the outward flow at saturation gives $N_m'=N_m/(1+\alpha)$. Assuming that the decay rate out of the lower-laser level is negligible, the satura-

tion population in the lower-lasing level is $N_n' = N_n + N_m\alpha/(1+\alpha)$. Using that the saturation intensity conditions are defined to occur when the gain is reduced to one-half the small-signal gain, the populations satisfy $(N_m' - N_n' h_m/h_n) = \frac{1}{2}(N_m - N_n h_m/h_n)$. Using this relation and the expressions for N_m' and N_n', we may thus determine α and the specific saturation intensity through Eq. (2):[23]

$$J_{\rm sat} = \left(\frac{h_n}{h_n+h_m}\right)\frac{\Gamma_0}{A_{mn}}\frac{2h\nu_{mn}^3}{c^2\sqrt{g_{mn}L_{\rm sat}}}. \tag{3}$$

The effect of gain narrowing is included by the addition of the $\sqrt{g_{mn}L_{\rm sat}}$ term, where $L_{\rm sat}$ is the lasing length required to reach saturation. The lower-lasing level influences the saturation intensity through the degeneracy h_n. This expression is valid when the lower-laser state does not have an exit channel. A very large lower-state degeneracy ($h_n \gg h_m$), has the same effect on $J_{\rm sat}$ as having a rapid exit channel out of the lower-laser state. However, when $h_n < h_m$ and there is no exit channel, there is a significant reduction in $J_{\rm sat}$ compared to the schemes with a rapid exit channel. For example, in H-like ions with lasing between the ground state and the first excited level $h_m = 8$ and $h_n = 2$ if fine structure is not included. The effect of not having a rapid exit channel out of the lower state results in a factor of 5 reduction in $J_{\rm sat}$ for H-like ions and a factor of $\frac{13}{4}$ for Li-like ions.

In general, one must also consider fine-structure effects on the specific saturation intensity, because the energy spacing between the fine-structure levels of interest are often greater than the linewidths of the lasing transitions. We assume that the fine-structure levels are populated according to their statistical weights. We have shown that this is a good approximation for lasing in Li-like Ne.[25] Let the fraction of the statistical weights of the upper (lower) levels that reside in the lasing level be f_m (f_n). Let N_n and N_m be the lower- and upper-lasing level populations. Now let Γ_0 be the averaged exit rate per atom in the upper shell. Following a similar procedure to the shell-averaged case, one finds a saturation intensity given by Eq. (3) increased by a factor of $1/f_m$. For the $2p_{3/2}$–$1s_{1/2}$ transition in H-like ions, this represents a factor of 2 increase in $J_{\rm sat}$, while for the $3d_{5/2}$–$2p_{3/2}$ in Li-like ions a factor of 3 is obtained. This effect is associated with the fact that the stimulated emission only operates on a fraction of the upper-shell population, while other processes, included through Γ_0, act on the entire upper-shell population.

The above analytic treatment assumes that the collisional rates are large enough that the populations can adjust on the gain duration time scale. We refer to this as the steady-state assumption. This assumption does not need to be made in the numerical treatment, where the equations for the level populations are calculated self-consistently, including collisional and stimulated emission terms. The stimulated terms are determined by solving the angle-averaged radiation transfer equation for the transition between the m and n levels:[7]

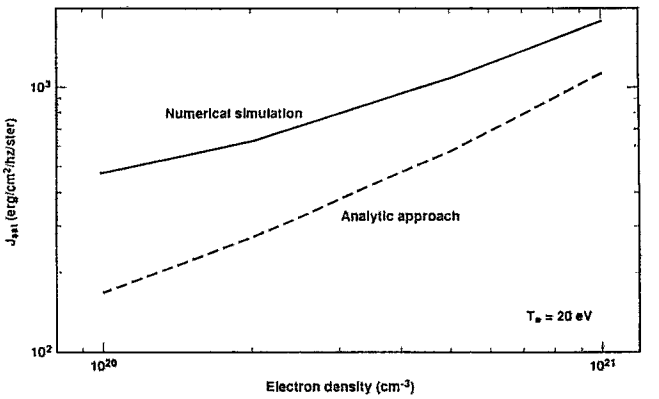

FIG. 1. Comparison of the analytical expression for $J_{\rm sat}$, including gain narrowing and a numerical solution for Li-like Ne lasing. The values are given for a range of densities at an electron temperature of 20 eV.

$$\frac{\partial\langle I_{mn}(y_l,z,t)\rangle}{\partial z} = \frac{g_{mn}(z,t)}{1+y_l^2}\left[\langle I_{mn}(y_l,z,t)\rangle + \Omega S_{mn}(z,t)\right], \tag{4}$$

where $\langle I_{mn}(y_l)\rangle = \int I_{mn}(y_l)\,d\Omega/4\pi$ is the angle-averaged specific intensity, Ω is a phenomenological solid-angle factor related to the geometry of the lasing medium, $S_{mn} = 2h\nu_{mn}^3 N_{mn}/\Delta N_{mn} c^2$ is the spontaneous emission source function, and $y_l = 2(\nu-\nu_{mn})/\Delta\nu_{mn}$ is the detuning parameter for the atomic line profile. This transfer equation is solved self-consistently with the population rate equations, which include the rates associated with Γ_0, other nonstimulated rates, and the stimulated rates associated with lasing transitions. The stimulated emission rate Θ_{mn} is related to the atomic-line-profile-weighted specific intensity $J_{mn} = \int dy_l \langle I_{mn}(y_l)\rangle/(1+y_l^2)$ through the standard Einstein relation: $\Theta_{mn} = J_{mn} A_{mn} c^2/2h\nu_{mn}^3$. To evaluate J_{mn}, we consider Eq. (4) beyond the spontaneous emission stage, i.e., $g_{mn} z > 1$, solve for $\langle I_{mn}(y_l,z,t)\rangle$, and carry through the integration over y_l by the method of steepest descents:

$$J_{mn}(z,t) = \langle I_{mn}(y_l=0,z,t)\rangle\sqrt{\pi}\left(\frac{e^{\tau(z,t)}-1}{(1+\tau(z,t))e^{\tau(z,t)}-1}\right)^{1/2}, \tag{5}$$

where $\tau(z,t) = \int^z dz'\, g_{mn}(z',t)$ is the gain length, and the range of integration extends only over amplifying regions, i.e., $g_{mn}(z',t) > 0$. In order to compare the analytical expression of $J_{\rm sat}$ with the numerical model for saturation, we use the lasing length $L_{\rm sat}$ determined from the numerical model. The comparison is given in Fig. 1 for a parameter space, where lasing in Li-like neon at 98 Å is calculated to have a high-energy efficiency ($E_{\rm out}/E_{\rm in} \geqslant 10^{-6}$), assuming beam propagation is not a problem.[6] The better agreement at higher densities is because the product of the gain duration and the collision frequency is an increasing function of density, which acts to validate the underlying steady-state assumption implicit in our analytic formulation.

The output energy at saturation is a product of the frequency- and angle-integrated intensity $I_{mn}(z,t)$

$\approx \Delta\nu_{mn} 2\pi J_{mn}$, the duration of lasing, and the cross-sectional area. The duration of lasing is determined by the filling of the lower-laser state, which scales as $1/A_{mn}$, except at high densities, where collisional filling is important. The fast radiative rates result in a gain duration of approximately 1–10 ps for the ions of interest. For confocal geometry, the output energy efficiency, $E_{\text{out}}/E_{\text{in}}$, does not depend on the cross-sectional area of lasing. We find that the energy efficiency is approximately 10^{-6} (comparable to conventional x-ray laser schemes) with significantly higher values possible if the driving laser can be focused for a number of saturation lengths.[5,6,8] Therefore, the predicted output energies of OFI x-ray lasers are in the μJ range given the input constraint of $E_{\text{in}} \leqslant 1$ J.

Although the output energy per pulse is low compared to conventional x-ray lasers, which have outputs in the mJ range, the OFI laser can operate at much higher repetition rates because of the smaller input energy requirements. Thus, OFI x-ray lasers can bridge the gap between conventional x-ray lasers and the quasicontinuous output of synchrotrons. With the recent advances in driving lasers, these three sources of coherent x rays can have comparable average power when operating at the narrow bandwidth ($\Delta\lambda/\lambda \approx 10^{-4}$), associated with x-ray lasers. Conventional x-ray lasers have large but relatively infrequent pulses that are appropriate for imaging biological objects[26] or for studying dilute short-lived samples, such as free clusters.[15] Synchrotrons are appropriate for looking at time-independent phenomena and where continuous tunability in wavelength is required. However, for many pump/probe and time-dependent experiments, a high repetition rate OFI x-ray laser would be a more useful and much less expensive x-ray source than a synchrotron. For example, an OFI x-ray laser would be an ideal tool for time-resolved photoelectron spectroscopy of surfaces. The discrete tunability, obtained by using different lasing ions, allows the study of different core levels. Continuous tunability, which is not currently available currently with x-ray lasers, is not required, because the energy of the ejected photoelectron is measured to determine the binding energy given a known photon energy. The photon energy is known accurately because of the narrow bandwidth of the x-ray laser. The number of photons per pulse is desired to be large, but below the limit associated with excessive space charge effects. The μJ OFI x-ray laser pulses provide the appropriate number of photons per pulse.[15] The above discussion gives the output properties of saturated OFI x-ray lasers and their potential applications. We now address potential problems and recent experiments.

B. Propagation issues and lasing in Li-like N

A potential problem for OFI plasma x-ray lasers is ionization-induced refraction associated with the confocal geometry. In general, as the laser is focused into a gas or plasma, the highest intensity is on the axis. This results in the highest degree of ionization, and therefore the largest electron density on axis. The electron density gradient in the transverse direction associated with the transverse intensity profile can result in a significant refraction of the ionizing pulse. The angle that a ray of the ionizing pulse bends after traveling a distance z is[27]

$$\Theta_R \approx \left(\frac{n_e}{n_c}\right) \frac{z}{L_D}, \tag{6}$$

where $n_c = \pi m_e (c/e\lambda)^2$ is the critical density, n_e is the electron density, $L_D = b^2/r(2 \ln 2)$ is the transverse intensity gradient scale length, and r is the transverse radial coordinate. We have assumed that n_e is proportional to the transverse intensity. Propagation calculations that self-consistently include the resulting electron density gradient and the effect of the transverse intensity profile changing, as a result of refraction and depletion of the pulse through ionization, are needed to more accurately address this problem. Keeping with our simple model, we identify an x-ray lasing length z_R with the distance a ray travels before its transverse displacement doubles. This length is found by setting $\Theta_R = r/z$, giving

$$z_R = b\sqrt{\frac{n_c}{n_e \ln 2}}.$$

The length does not depend on r for the assumed Gaussian transverse intensity profile or for any other profile that is a function of r^2.

A simple solution for the problem of ionization-induced refraction is to use a larger focal spot size.[8] For a given amount of driving laser energy, this means a drop in intensity and the necessity of choosing an element with a lower ionization potential. Here Li-like N with lasing at 247 Å requires an intensity of approximately 3×10^{16} W cm^{-2} to achieve the required ionization using a 100 fs duration pulse. Only 150 mJ is required for a spot size of 40 μm, which for a peak electron density of 5×10^{19} cm^{-3}, and a driving wavelength of 0.25 μm gives a lasing length of approximately 2 mm with refraction. For an electron temperature of 10 eV, we calculate a gain coefficient of approximately 30 cm^{-1}. This would give a gain-length product of 6, which would be more than a factor of 100 above spontaneous emission.[8] A plot of the ratio of lasing emission to spontaneous emission for two different densities and a range of laser beam waist radii is shown in Fig. 2 for an electron temperature of 10 eV. A beam waist radius of 40 μm should provide clear evidence of Li-like N lasing for densities of order 2.5×10^{19} cm^{-3} and higher provide the electron temperature is 10 eV or less.

It is possible that the problem of ionization-induced refraction can be solved by other means. One approach is to obtain a very flat transverse intensity profile, or even one with a local minimum on axis. There has been some success with this approach, but at lower densities than required for OFI lasing.[28] Another approach is to create a plasma channel with a minimum in the density on axis prior to field ionization. Recent experiments show that this approach has some promise.[29] The major question with creating a channel is whether the required initial conditions of moderate density and low temperature can be obtained inside the channel.

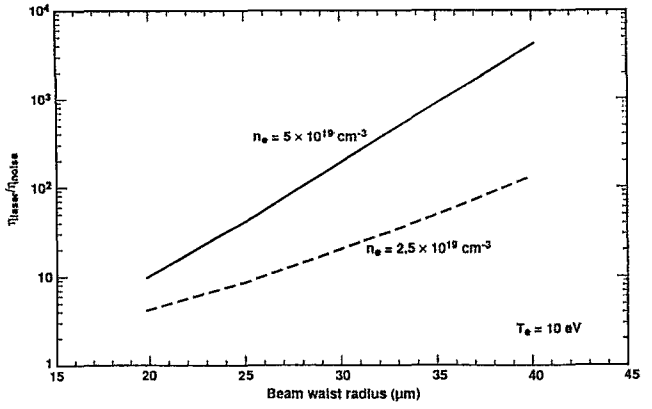

FIG. 2. Ratio of stimulated emission to spontaneous emission at 247 Å versus beam waist radius for an electron temperature of 10 eV in Li-like N.

C. Calculation of electron heating

A low ambient electron temperature following field ionization is critical for the success of the OFI x-ray laser scheme. Field ionization has the potential of leaving the ionized electrons with relatively little energy, because electrons ionized near the peak of the slowly varying laser electric field return the majority of their large oscillatory energy back to the field as the pulse leaves the plasma. Since the ionization rate is a strong function of the electric field, the majority of the ionization occurs near the peak of the field. The heating associated with the energy that the electrons do not return to the laser field is referred to as above-threshold-ionization (ATI) heating, and has been considered by a number of authors.[3,21,22,30] The amount of energy associated with the phase mismatch between the instant of ionization and the peak of the oscillatory electric field depends on the oscillation or quiver velocity of the electron, and hence on the wavelength of the applied laser. In all calculations of ATI, a clear benefit is predicted in using shorter wavelengths for the ionizing pulse. Recent experiments using a laser operating at 0.8 μm to ionize low-density He (7×10^8 atoms/cm^3) measured the ATI energy spectrum.[31] A single temperature fit to the data gives 30 eV, which is comparable to the ionization potential of 24.6 eV. In this case, rapid recombination and lasing is not expected. In addition to using shorter wavelengths, space-charge effects can reduce ATI for some densities, as indicated by particle-in-cell (PIC) simulations.[8,22] A calculation of ATI[8] for ionizing N to a He-like ion with 0.25 μm radiation, an intensity of 3×10^{16} W/cm^2, and a pulse duration of 100 fs found an electron temperature of order 20 eV for low density, but less than 1 eV for gas densities near 10^{18} atoms/cm^3. However, this calculation is for a 1 μm laser focal spot and a higher ATI would be expected for larger focal spots. Additional experiments and theory are needed to address ATI at densities and focal spot sizes appropriate for lasing.

Collisions by the rapidly oscillating electrons is another source of electron heating during field ionization which can be estimated by taking the electron quiver energy and multiplying by an electron–ion collision frequency.[22,30] However, there are differences in the choice of the Coulomb logarithm $\ln\Lambda$ used in the different calculations.[8] For example, the calculations of Rae and Burnett[30] predict that collsional heating is a major problem, but they did not include the correction for the large ratio of laser frequency to plasma frequency,[32] which can result in a large overestimate for the heating. In contrast, the calculations of Penetrante and Bardsley[22] predict that collisional heating is not a problem, but their use of a kinetic description based on the high-Z analysis of Jones and Lee[33] is uncertain for the low-Z elements of interest. In addition, for some plasma parameters there is a low number of particles in a Debye sphere, e.g., $T_e=10$ eV and $n_e=5\times10^{19}$ cm^{-3} in He-like N gives seven particles.[8] In this case, the Debye length is a less accurate measure of the maximum impact parameter. Additional work including velocity anisotropy and electron–electron collisions is desired to address this source of heating.

Heating associated with stimulated Raman backscatter is a major problem in extending the OFI approach to shorter wavelengths by using ions with higher ionization potentials. For Li-like Ne with lasing at 98 Å, the use of a short duration pulse ($\Delta t\leqslant100$ fs) was shown to be sufficient to limit the growth of Raman backscatter.[5,6] For Li-like Al with lasing at 52 Å, the combination of a need for a higher laser intensity ($I=1\times10^{18}$ W/cm^2), and a higher electron density ($n_e=1\times10^{21}$ cm^{-3}) resulted in a calculated electron temperature of order 1 keV from Raman heating for a 50 fs pulse.[6] The use of a shorter pulse to reduce Raman is not practical because there is not sufficient energy in the pulse to ionize the plasma to He-like Al over a suitably large volume.

In conclusion, some experiments and theoretical calculations indicate electron heating is a major problem for OFI lasing, while others indicate that heating can be control using appropriate target and driving laser parameters. Additional experiments and calculations that are in progress or are being planned will help in resolving issues associated with this important aspect of OFI lasing.

D. Recent experiments in H-like Li

Recent experiments at the RIKEN laboratory in Japan observed faster than linear growth with increasing lasing length for the $2p\rightarrow1s$ or L_α transition at 135 Å in H-like Li following field ionization by a 500 fs KrF laser operating at 0.25 μm.[34] These experiments are potentially the first demonstration of OFI lasing at x-ray wavelengths. A fit of their intensity versus length gave a gain coefficient of 20 cm^{-1}, giving a gain-length product of 4 for their maximum length of 2 mm. The observation of the time dependence of an OFI x-ray laser intensity provides important information. Lasing is expected immediately after the pump pulse, with a duration of order 10 ps for H-like Li. Therefore, one would expect to observe a spike of emission of this duration followed by spontaneous emission associated with continued recombination. The initial RIKEN experiments were time integrated, but ongoing experiments at RIKEN are trying to measure the time dependence of the emission.

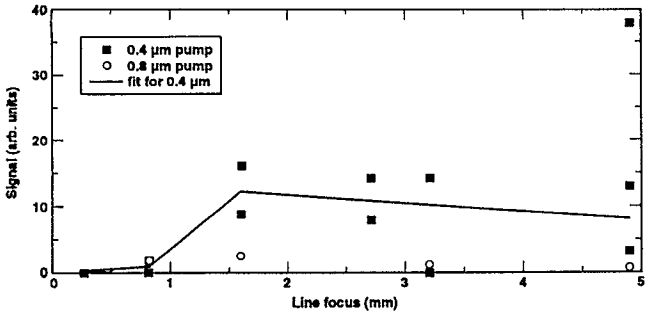

FIG. 3. The intensity versus length for the L_α 135 Å transition in H-like Li for ionization of the ablated Li by the 100 fs Ti: Sapphire at 0.8 and 0.4 μm wavelengths.

We have attempted to duplicate the RIKEN experiments using a 100 fs Ti-Sapphire laser located at the University of California campus in Berkeley.[35] As at RIKEN, the plasma is obtained by laser ablation of a solid Li target and ionized by the high-intensity short-pulse laser. The laser intensity is approximately 2×10^{17} W/cm^2, and it is operated at both the fundamental wavelength of 0.8 μm and the second harmonic at 0.4 μm. The time dependence of the emission is measured with a streak camera.[36] The intensity as a function of length for the L_α transition at 135 Å in H-like Li is shown in Fig. 3. For ionization using the second harmonic, faster than linear growth is observed out to a length of 1.5 mm, with large scatter in the data for longer lengths with no evidence of continued nonlinear growth. Nonlinear growth is not observed for any lengths when the fundamental wavelength is used to ionize the Li. A fit of the data using the second harmonic out to 1.5 mm gives a gain coefficient of approximately 30 cm^{-1} and a gL of 4.5, which is comparable to what was measured at RIKEN. Propagation problems, as discussed in Sec. II B, are believed to the major impediment in achieving lasing at longer lengths and thus obtaining larger gain-length products.

The time dependence of the 135 Å emission is shown in Fig. 4 for a length of 1.5 mm, along with calculations for the spontaneous emission for two different temperatures.

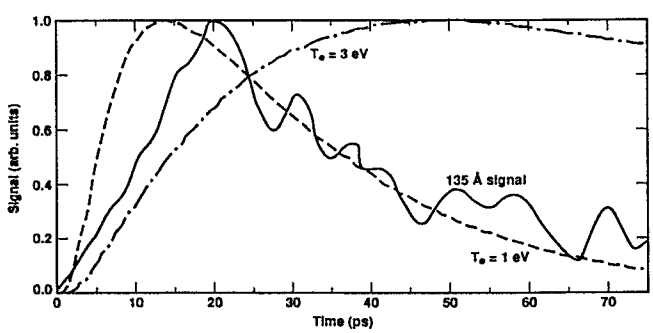

FIG. 4. The observed time dependence for the L_α 135 Å transition in H-like Li for a length of 1.5 mm. Time resolution of the camera is 15 ps for this data. Calculations of spontaneous emission during recombination for an electron density of 5×10^{18} cm^{-3}, and electron temperatures of 1 and 3 eV are shown.

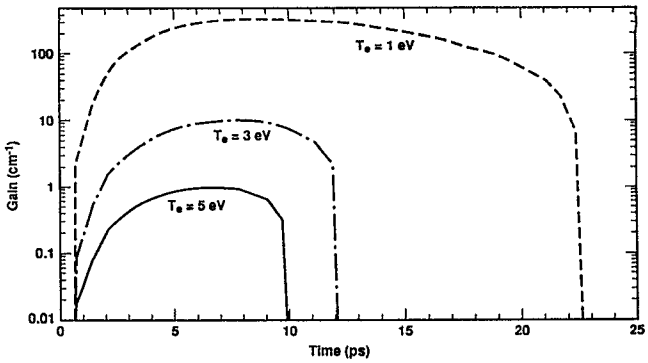

FIG. 5. The calculated gain coefficients for the L_α 135 Å transition in H-like Li for an electron density of 5×10^{18} cm^{-3} and electron temperatures of 1, 3, and 5 eV are shown.

The figure suggests both good news and bad news for the possibility of OFI lasing. The good news is that the time scale for recombination is very short, which implies a low electron temperature and the possibility of large gain coefficients. The bad news is that we do not observe a large spike of emission at the beginning of the recombination, as would be expected for a gain-length product of order 4. This apparent contradiction between the length-study data and the time-resolved data underscores the need to achieve longer lasing lengths. The modeling curves in Fig. 4 give only the spontaneous emission during recombination for an electron temperature of 1 and 3 eV at an assumed electron density of 5×10^{18} cm^3. The lower temperature gives the best fit to the observed recombination time scale. A temperature of 1 eV is significantly below what is expected from ATI heating.[22] One possible explanation is that the removal of the outer Li electron, with an ionization potential of 5.4 eV, should be treated as two-photon ionization rather than field ionization. The photon energy for 0.4 μm light is approximately 3 eV, which would result in the outer electron having an energy of order 1 eV following ionization. Another explanation is that Li did not fully recombine after laser ablation (prior to field ionization), with the remaining free electrons at a low initial temperature. The potential problem with these explanations is that the electron–electron collision time is of order 1 ps, so that one would expect significant thermalization of the 1 eV electrons with the higher-energy field-ionized electrons. A question we are addressing is whether there are a sufficient number of low-energy electrons available to have the observed rapid recombination.

The rapid recombination does indicate that the plasma conditions are appropriate for lasing. In Fig. 5 we show the calculated gain coefficients for $n_e=5\times10^{18}$ cm^{-3} and $T_e=1$, 3, and 5 eV. The maximum gain for 1 eV is over 100 cm^{-1}, while the maximum gain for 3 eV is over 10 cm^{-1}. At this time, we do not have an independent measurement of electron density. While a higher electron density would allow a higher electron temperature to match the recombination time scale, the gain coefficient in this scenario would also be high. Conversely, if the electron density is lower than the assumed 5×10^{18} cm^{-3}, the observed rapid

recombination would imply an electron temperature less than 1 eV with a corresponding high gain coefficient. The conclusions that can be drawn at this time are that there is some evidence for lasing over short lengths, that the observed fast recombination time indicates that the plasma has appropriate conditions following ionization to have high gain coefficients, and that propagation of the ionizing laser pulse is a potential problem.

III. INNER-SHELL PHOTOIONIZATION SCHEME

Inner-shell photoionization pumping was one of the first x-ray laser schemes suggested.[9] The approach we discuss involves a high-intensity short-pulse laser heating a high-Z target, e.g., Au, which emits a pulse of incoherent x rays.[10] After filtering, the remaining hard x rays preferentially photoionize inner-shell electrons creating a transient population inversion in the lasant material. The scheme is of interest because it offers the possibility of lasing with wavelengths from 15 down to 5 Å using elements from Ne to Cl. The upper-laser state corresponds to an electron hole in the inner K shell and the lower-laser state corresponds to an electron missing from the outer L shell. The energy of the required x rays for inner-shell ionization ranges from 870 eV up to 2.8 keV for the elements of interest (Ne to Cl). A high-intensity driver is needed because a large x-ray flux is required to maintain an upper-laser state population given the very rapid Auger decay process. The short duration driving pulse is required to ensure a rapid rise time for the x rays because the lower-laser state is populated primarily by electron collisional ionization of the neutral atoms, which in a short time destroys the population inversion. The addition of H as an electron moderator in the lasant material has been suggested as a way to mitigate electron collisional ionization.[10,11] We briefly discuss the role of low-energy filters and electron moderators. Following a discussion of I_{sat} for ISPI x-ray lasers, we discuss what experiments can be conducted with existing lasers.

A. Low-energy filters and electron moderators

Population inversion is possible for ISPI x-ray lasers because the photoionization cross section is an order of magnitude higher for inner-shell electrons, as compared to outer-shell electrons at photon energies just above the inner-shell binding energy. However, population inversion requires that photons with energy below this binding energy be filtered because they would only populate the lower-laser state. The optimum filter material and thickness depends on the spectrum of the incoherent x rays and the lasant material, but we have found that filters made of Li, Be, or B with a thickness of 2–5 μm are effective in blocking the low-energy x rays, with only a minimal reduction of higher-energy x rays that can ionize inner-shell electrons.

Electron collisional ionization of outer-shell electrons is a problem that is more difficult to control than photoionization by low-energy x rays. Collisional ionization can directly populate the lower-laser state or indirectly reduce the population inversion because of a reduction in the neutral population that feeds the upper-laser state. The second effect becomes more important for the higher-Z lasant materials that have many M-shell electrons. The electrons come from photoionization and Auger decay. One approach to mitigate this problem is the introduction of a large amount of H in the lasant material.[10] Compared to the lasant materials, the photoionization cross section for H is many order of magnitudes lower, while the collisional cross sections for ionization and excitation of H are comparable. With the appropriate concentration of H, the majority of the x rays are absorbed by the lasant material, and most of the electron kinetic energy is absorbed by H. Calculations have used 1% Ne in a solid H_2 target[10] and 15% Mg in H at a H density of 1×10^{21} cm^{-3} ($\approx$0.1, solid),[11] giving gain coefficients in each case of order 10 cm^{-1}. For the Ne calculation, a reduction in gain of order 30% is found without using an electron moderator. In Mg the electron moderator is more important, where a factor of 10 reduction is found without using H. A mixture of LiH with a small fraction of lasant material would provide the necessary H for experiments using a spot focus discussed in Sec. III C and would avoid the need for cryogenic targets. However, for lasing experiments using a line focus, the absorption by Li of the lasing photons is a problem.

B. Saturation intensity and output energy for ISPI schemes

Following a procedure of equating population flows with and without stimulated terms, as discussed for OFI lasers, one obtains the following expression for the saturation intensity:[23]

$$J_{sat}=\frac{2P_{01}}{P_{02}}\frac{\Gamma_0}{A_{21}}\frac{2h\nu^3}{c^2\sqrt{g_{21}L_{sat}}}, \tag{7}$$

where P_{02} is the inner-shell photoionization rate from the neutral atom (level 0) to the upper-laser state (level 2), P_{01} is the combination of the collisional and photoionization rates to the lower-laser state (level 1), Γ_0 is the outward flow rate out of level 2, including all nonstimulated processes, and $\sqrt{g_{21}L_{sat}}$ is included to account for gain narrowing. The Auger rate out of level 2 is always the dominant process included in Γ_0. In this calculation of J_{sat}, the exit rate out of the lower-laser level is assumed small, as in the case for OFI lasing. We find the interesting result that J_{sat} increases with increasing pumping to the lower-laser state. A larger P_{01} results in a faster filling of the lower-laser state and an earlier time of maximum gain. However, the value of the maximum gain is inversely proportional to P_{01} making it more difficult to reach saturation with increasing P_{01}. The value of J_{sat} is important for some applications, while for others the output energy is important. To obtain the output energy, J_{sat} is multiplied by the frequency width $\Delta\nu$, the viewing solid angle 2π, the duration of lasing Δt, and the cross-sectional area A of the lasing volume. The line width is primarily determined by the natural width associated with the short time scale for Auger decay of the upper-laser state $\Delta\nu\approx\Gamma_0/2\pi$. To de-

termine the duration of lasing, we use the FWHM duration of the gain. For pumps that increase linearly in time and for $A_{21}/\Gamma_0 \ll P_{01}/P_{02}$,

$$\Delta t = \frac{\sqrt{2}h_1}{h_2}\frac{P_{02}}{P_{01}}\frac{1}{\Gamma_0}.$$

Using these with Eq. (7) and $\sqrt{g_{21}L_{\text{sat}}} \approx 4$, the output energy at saturation is given approximately by

$$E_{\text{out}} = \frac{h_1}{\sqrt{2}h_2}\frac{\Gamma_0}{A_{21}}\frac{2h\nu^3}{c^2}A. \tag{8}$$

For the case of lasing on the $2p \rightarrow 1s$ transition at 14.6 Å in neon, and assuming the cross-sectional area of the lasing volume is 5 μm^2, one has $E_{\text{out}} = 0.4$ μJ. Our recent calculations suggest that gains of order 15 cm^{-1} are possible using a driving laser with an intensity of 10^{17} W/cm^2 and a pulse duration of 100 fs focused onto an area 5 μm wide by 1 cm long.[11] The input energy is 5 J, giving an energy efficiency of approximately 10^{-7}. This efficiency is about a factor of 10 less than conventional or OFI x-ray lasers. If higher gains are obtained, saturation would occur for lengths less than 1 cm, giving higher efficiencies. In addition, the lower-laser state does have a finite exit rate associated with inner-shell ionization of the remaining K-shell electron, and for Mg and higher Z elements the lower-laser state can Auger decay. Including these, exit rates would serve to increase J_{sat} above the value used beyond to determine E_{out} used in Eq. (8).

C. Possible ISPI experiments using existing lasers

A line focus of order 1 cm is not possible with existing lasers, given the need for intensities of order 10^{17} W/cm^2 and a corresponding energy of 5 J and greater. However, there are important nonlasing experiments that can be conducted using a spot focus and existing lasers. It has been shown that structured targets with surface grooves or made from a composite of clusters, e.g., gold black, have higher absorption of short pulses than planar targets and can generate a larger number of the hard x rays that are needed for inner-shell ionization.[37] We model grooved targets as an ensemble of planar exploding foils and find that a rise time of x rays appropriate for inner-shell ionization of Ne, with lasing at 14.6 Å, can be obtained from Au targets heated by 100 fs pulses.[11,38] Additional experiments that measure the spectrum and time dependence of x rays emitted from targets heated by short-pulse lasers are desired.

Experiments using a spot focus can also address important kinetic issues for ISPI x-ray lasers. For example, in Mg there is a rapid Auger decay of the $2s$ hole state. The lower-laser state is a $2p$ hole and there is a question of whether these two states are in thermal equilibrium via electron and ion collisions. Experiments that measure the ratio of the potential lasing transition, $1s$ hole to $2p$ hole in singly ionized Mg, to the three corresponding transitions in doubly ionized Mg, where there is an additional electron hole in the $2s$, $2p$, or $3s$ level can provide information on thermalization of the $2s$ and $2p$ hole states. Our calculations predicted more than a factor of 2 difference in the ratio of the transition with an additional $2p$ hole to the lasing transition, depending on how large the collisional rate is that connects the $2s$ and $2p$ hole states. Information about the ratio of photo pump rates and collisional rates can be obtained from these line ratios. In addition, spot focus experiments can address the question of optimum low-energy filter material and thickness, as well as the role of H in slowing down Auger electrons that can collisionally populate the lower-laser level.[10,11]

IV. SUMMARY

Optical-field-ionized plasma x-ray lasers appear to be a potential path for achieving low-cost tabletop size x-ray lasing. We calculated that the expected output of OFI lasers are μJ pulses at a high repetition rate and that such a laser would find many applications. We discussed a design for lasing in Li-like N at 247 Å that addresses the issue of ionization-induced refraction. Clear evidence of lasing in N is calculated for electron densities above 2.5×10^{19} cm^{-3} using an input energy of only 150 mJ, provided the electron temperature is of order 10 eV. The question of the electron temperature following field ionization is not clear at this time, with significant differences obtained in the different calculations. There are questions of how much space-charge effects can reduce ATI heating and the amount of collisional heating expected for the low Z ions of interest. Recent time-resolved experiments in H-like Li indicate rapid recombination requiring very low temperatures ($T_e \approx 1$ eV). These experiments and similar time-integrated data at RIKEN show faster than linear growth up to lengths of order 2 mm for the L_α 135 Å transition in H-like Li. Propagation is a potential problem in extending the lasing length in this system. Experiments and theoretical work are in progress to address this issue.

Inner-shell photoionization x-ray lasers can operate at very short wavelength, but demonstration of lasing requires more energy than is available from current drivers. However, there are many experiments that can be conducted with existing lasers that test different aspects of this approach to lasing.

ACKNOWLEDGMENTS

This work was performed under the auspices of the U.S. Department of Energy by the Lawrence Livermore National Laboratory under Contract No. W-7405-ENG-48.

[1] L. I. Gudzendko and L. A. Shelepin, Zh. Eksp. Teor. Fiz. **18**, 998 (1964) [Sov. Phys. Dokl. **10**, 147 (1965)].
[2] W. W. Jones and A. W. Ali, Appl. Phys. Lett. **26**, 450 (1975).
[3] N. H. Burnett and P. B. Corkum, J. Opt. Soc. Am. B **6**, 1195 (1989).
[4] N. H. Burnett and G. D. Enright, IEEE J. Quantum Electron. **26**, 1797 (1990).
[5] P. Amendt, D. C. Eder, and S. C. Wilks, Phys. Rev. Lett. **66**, 2589 (1991).
[6] D. C. Eder, P. Amendt, and S. C. Wilks, Phys. Rev. A **45**, 6761 (1992).
[7] P. Amendt, D. C. Eder, R. A. London, and M. D. Rosen, Phys. Rev. A **47**, 1572 (1993).
[8] P. Amendt, D. C. Eder, R. A. London, B. M. Penetrante, and M. D. Rosen, *SPIE Proceedings*, Conference on Short-Pulse High-Intensity

Lasers and Applications, Los Angeles, 1993, edited by H. A. Baldis (SPIE, Bellingham, WA, 1993), Vol. 1860, p. 140.
[9]M. A. Duguay and P. M. Rentzepis, Appl. Phys. Lett. **10**, 350 (1967).
[10]H. Kapteyn, Appl. Opt. **31**, 4931 (1992).
[11]G. L. Strobel, D. C. Eder, R. A. London, M. D. Rosen, R. W. Falcone, and S. P. Gordon, in Ref. 8, p. 157.
[12]*X-Ray Lasers* 1992, Proceedings of the 3rd International Colloquium on X-Ray Lasers, IOP Conference Series 125, edited by E. E. Fill (Institute of Physics, Bristol, England, 1992).
[13]L. A. Hackel, J. L. Miller, and C. B. Dane, Int. J. Nonlinear Opt. Phys. **2**, 171 (1993).
[14]M. V. Ammosov, N. B. Delone, and V. P. Krainov, Zh. Eksp. Teor. Fiz. **91**, 2008 (1986) [Sov. Phys. JETP **64**, 1191 (1986)].
[15]D. C. Eder, P. Amendt, C. B. Dane, L. B. Da Silva, L. A. Hackel, M. R. Hermann, R. A. London, B. J. MacGowan, D. L. Matthews, M. D. Rosen, and S. C. Wilks, *Proceedings of the 5th International Conference on Lasers and Applications*, Houston, TX, 1992, edited by C. P. Wang (STS Press, McLean, VA, 1993).
[16]E. J. Valeo and S. C. Cowley, Phys. Rev. E **47**, 1321 (1992).
[17]S. Basu, P. L. Hagelstein, J. J. Goodberlet, M. H. Muendel, and S. Kaushik, Appl. Phys. B **57**, 303 (1993).
[18]J. J. Rocca, E. E. Beethe, and M. C. Marconi, Opt. Lett. **13**, 565 (1988).
[19]C. Steden and H. J. Kunze, Phys. Lett. A **151**, 534 (1990).
[20]*SPIE Proceedings*, Ultrashort-Wavelength Lasers II, San Diego, CA, 1993, edited by S. Suckewer (SPIE, Bellingham, WA, 1994), Vol. 2012.
[21]P. B. Corkum, N. H, Burnett, and F. Brunel, Phys. Rev. Lett. **62**, 1259 (1989).
[22]B. M. Penetrante and J. N. Bardsley, Phys. Rev A **43**, 3100 (1991).
[23]G. L. Strobel, D. C. Eder, and P. Amendt, Appl. Phys. B **58**, 45 (1994).
[24]R. W. Lee, J. Quant. Spectrosc. Radiat. Transfer **40**, 561 (1988).
[25]D. C. Eder, P. Amendt, M. D. Rosen, J. K. Nash, and S. C. Wilks, *Proceedings on Short-Wavelength Coherent Radiation*, Monterey, CA, 1991, edited by P. H. Bucksbaum and N. M. Ceglio (Optical Society of America, Washington, DC, 1991), Vol. 11, p. 96.
[26]L. B. DaSilva, J. E. Trebes, R. Balhorn, S. Mrowka, E. Anderson, D. T. Attwood, T. W. Barbee, Jr., J. Brase, M. Corzett, J. Gray, J. A. Koch, C. Lee, D. Kern, R. A. London, B. J. MacGowan, D. L. Matthews, and G. Stone, Science **258**, 269 (1992).
[27]W. P. Leemans, C. E. Clayton, W. B. Mori, K. A. Marsh, P. K. Kaw, A. Dyson, and C. Joshi, Phys. Rev. A **46**, 1091 (1992).
[28]A. Sullivan, H. Hamster, S. P. Gordon, H. Nathel, and R. W. Falcone, in Ref. 20.
[29]C. G. Durfee, III and H. M. Milchberg, Phys. Rev. Lett. **71**, 2409 (1993).
[30]S. C. Rae and K. Burnett, Phys. Rev. A **46**, 2077 (1992).
[31]U. Mohideen, M. H. Sher, H. W. K. Tom, G. D. Aumiller, O. R. Wood II, R. R. Freeman, J. Bokor, and P. H. Bucksbaum, Phys. Rev. Lett. **71**, 509 (1993).
[32]I. P. Shkarofsky, T. W. Johnston, and M. P. Bachynski, *The Particle Kinetics of Plasmas* (Addison–Wesley, Amsterdam, 1966), p. 260.
[33]R. D. Jones and K. Lee, Phys. Fluids **25**, 2307 (1982).
[34]Y. Nagata, K. Midorikawa, M. Obara, H. Tashiro, and K. Toyoda, Phys. Rev. Lett. **71**, 3774 (1993).
[35]M. M. Murname and R. W. Falcone, J. Opt. Soc. Am B **5**, 1573 (1988).
[36]M. M. Murname, H. C. Kapteyn, and R. W. Falcone, Appl. Phys. Lett. **56**, 1948 (1990).
[37]M. M. Murname, H. C. Kapteyn, S. P. Gordon, J. Bokor, E. N. Glytsis, and R. W. Falcone, Appl. Phys. Lett. **62**, 1068 (1993).
[38]D. C. Eder, G. L. Strobel, R. A. London, and M. D. Rosen, *SPIE Proceedings*, Applications of Laser Plasma Radiation, San Diego, CA, 1993, edited by M. Richardson (SPIE, Bellingham, WA, 1994), Vol. 2015, p. 234.